RAPID COMMUNICATION

Transport Properties in a Single Domain of Microscale Sr$_2$RuO$_4$ Single Crystals

Hiroyoshi Nobukane*, Katsuhiko Inagaki, Satoshi Tsuchiya, Yasuhiro Asano, Koichi Ichimura, Kazuhiko Yamaya, Shigeru Takayanagi, Ikuto Kawasaki[1], Kenichi Tenya[2], Hiroshi Amitsuka[1], and Satoshi Tanda

Department of Applied Physics, Hokkaido University, Sapporo 060-8628, Japan
[1]*Department of Physics, Hokkaido University, Sapporo 060-0810, Japan*
[2]*Department of Education, Shinshu University, Nagano 380-8544, Japan*

We report our approach to measuring the transport properties in a single chiral order parameter domain of microscale Sr$_2$RuO$_4$ single crystals. Sr$_2$RuO$_4$ single crystals were grown by the solid-phase reaction. Microscale single crystals were deposited from a dispersed liquid, and selected from the result of the chemical composition and crystallinity of the dispersed crystals. The selected crystals attached to gold electrodes show superconducting properties. We also found the anomalous current–voltage characteristics that show that induced voltage is an even function of bias current. © 2010 The Japan Society of Applied Physics

Anisotropic superconductors[1–3] stimulate much interest in a nontrivial order parameter field, but have domain configurations due to the internal degrees of freedom of the order parameter. The size of a single domain is considered to be on the micro–nanoscale. In Sr$_2$RuO$_4$,[4] which is a promising candidate of spin-triplet chiral p-wave superconductor (i.e., spin $S = 1$ and orbital angular momentum $L = 1$), polar Kerr effect measurements[5] and Josephson tunneling measurements[6] suggested the single chiral domain sizes to be $1-50\,\mu m$. The coherence length of Sr$_2$RuO$_4$ is $\xi_{ab}(0) = 66\,nm$ in the ab-plane. The experimental data of Sr$_2$RuO$_4$ on the millimeter scale should be considered as a result of ensemble-averaging over possible chiral domain configurations. Hence, transport measurements of a microscale Sr$_2$RuO$_4$ crystals are very important in both fundamental studies and potential applications for realizing topological quantum computation.[7] Recently, a microfabrication technique using a focused ion beam has been reported for Sr$_2$RuO$_4$–Ru eutectic systems.[8] Since such eutectic systems show $3\,K$ phase superconductivity to be inhomogeneous and filamentary,[4,9] we need a microscale Sr$_2$RuO$_4$ crystal with no ruthenium inclusion in order to study phenomena peculiar to a single chiral domain. However, experiments on microscale pure crystals of Sr$_2$RuO$_4$ are still limited.[10]

In this paper, we report our approach to measuring the transport properties in a single chiral order parameter domain of microscale Sr$_2$RuO$_4$ single crystals. For microscale Sr$_2$RuO$_4$ crystals with no ruthenium inclusion nor impurities as determined from the results of analyses, electrical contact was formed by welding using electron beam irradiation. The transition temperature of the Sr$_2$RuO$_4$ single crystals was consistent with the result for bulk Sr$_2$RuO$_4$. Moreover, we found that the induced voltage V is an even function of the bias current I, while V is usually an odd function of I in four terminal measurements.

In micro-nanofabrication methods, it is necessary to solve two essential issues: crystallinity and electrical contact. The first concerns the degradation of the crystallinity of microscale superconducting samples. Nanofabrication techniques for the epitaxial growth of nanoscale cuprates have been reported.[11] These epitaxial methods cause problems of grain
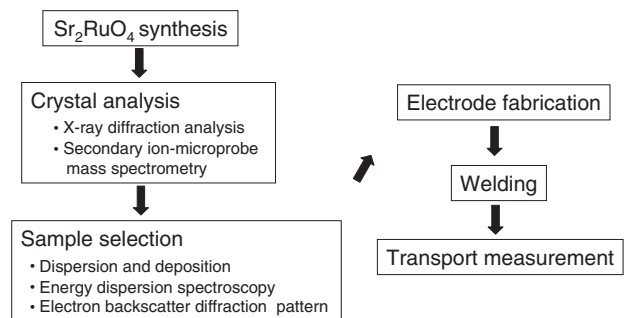
Fig. 1. Procedure from the synthesis of Sr$_2$RuO$_4$ to transport measurements.

formation. The second concerns the difficulty in the formation of an electrical contact.[9] The surface of a cleaved crystal may have an insulator layer, and a poly(methyl methacrylate) (PMMA) resist may also remain between the sample and the gold electrodes. Therefore, electron beam lithography, which is used to study carbon nanotubes and graphene, cannot be applied directly to layered crystals. Considering these issues, we selected microscale single crystals from among dispersed crystals and welded them to gold electrodes by electron beam irradiation in order to measure transport properties. Figure 1 shows the procedure from sample growth to transport property measurements. Sr$_2$RuO$_4$ single crystals were synthesized by the solid-phase reaction. Microscale single crystals were deposited from a dispersed liquid, and selected from the chemical composition and crystallinity of the dispersed microscale crystals. For the selected samples, they were firmly attached to gold electrodes and then heated by electron beam irradiation to improve contact resistance. In the following paragraphs, we will describe this procedure in detail.

For the growth of microscale Sr$_2$RuO$_4$ single crystals, we used the solid-phase reaction. We prepared SrCO$_3$ and RuO$_2$ (both 99.9% pure, Kojundo Chem.) powders. Firstly, the powder mixture, which had a total weight of $10\,g$, was placed in a furnace at $400\,°C$ for $4\,h$ to exclude CO$_2$ gas. The mixed powder was then sintered in Al$_2$O$_3$ boats in air at $990\,°C$ for $60\,h$. The mixture was cooled gradually from 990 to $450\,°C$ over $6\,h$. The samples were kept at $450\,°C$ for $12\,h$ to introduce oxygen into the crystals and then cooled slowly to room temperature. After grinding and pressing, the

*Present address: Department of Physics, Asahikawa Medical College, Asahikawa, Hokkaido 078-8510, Japan.

samples were sintered again at $1070\,°C$ for $60\,h$. We removed the sample surface in contact with the Al_2O_3 boats.

We determined the crystal structure of Sr_2RuO_4 and the concentration of impurities. X-ray diffraction analysis was used to determine the structure of the Sr_2RuO_4 crystals. The observed peaks were fitted to a body-centered tetragonal unit cell of the K_2NiF_4 type with the lattice constants $a = b = 3.867$ (±0.004) Å and $c = 12.73$ (±0.01) Å.[12] Since the superconductivity of Sr_2RuO_4 is destroyed by nonmagnetic and magnetic impurities,[13] we performed a detailed analysis of impurities using secondary ion-microprobe mass spectrometry (SIMS) for the samples in the same batch with the measured microscale Sr_2RuO_4. The result of the SIMS shows that the concentration of the Al in the sample is less than $100\,ppm$.

We selected microscale Sr_2RuO_4 single crystals on the basis of the results of the chemical composition and crystallinity. The samples were dispersed in dichloroethane by sonication for $30\,min$ and deposited on an oxidized Si substrate where thick gold markers and contact pads had been inscribed. As another technique in which microscale crystals are put on substrates,[14] the mechanical exfoliation of Sr_2RuO_4 crystals on substrates was performed successfully. We observed typical samples about $50\,nm$ to $500\,\mu m$ in length. Energy dispersion spectroscopy (EDS; JEOL EX-641750JMU) was used to determine the components of the microscale samples on the substrate. The atomic ratio of Sr to Ru elements was $2:1$, which was consistent with that of the bulk crystal. We also confirmed that the dispersed crystals had no boundaries nor ruthenium inclusions on the sample surface by observing the crystal orientation using an electron backscatter diffraction pattern (EBSP; OIM TSL[15]). Figure 2 shows the result of the EBSP. By this technique, the crystal orientation is represented as a color variation (see the inset of Fig. 2). The red region indicates that the crystal orientation is in the same direction. In other words, the microscale Sr_2RuO_4 shows single crystals in the *ab*-plane. Thus, the EBSP method is efficient in proving that the grown crystals are single crystals on the microscale.

On the analyzed samples, we fabricated gold electrodes by overlay e-beam lithography and then performed local welding by electron beam irradiation. Figure 3(a) shows a micrograph of the microscale Sr_2RuO_4 (sample B). Here, the size of sample A is $13.0 \times 6.67 \times 0.34\,\mu m^3$. The size of sample B is $2.50 \times 1.88 \times 0.10\,\mu m^3$. The spacings between the voltage electrodes are $4.0\,\mu m$ (sample A) and $0.63\,\mu m$ (sample B). In lithography, the PMMA resist was $1.4\,\mu m$ thick in bilayers. Lift-off was performed with acetone at room temperature for $3\,h$, and then in boiling acetone for $30\,min$. Since the fabricated sample surface may have an insulator surface of layered crystals and a residual PMMA resist between the sample and the gold electrodes, it is difficult to form electrical contact. In order to solve these problems, welding is performed. Figure 3(b) shows schematic of welding. We locally heated each electrode on the samples for $15\,s$ by irradiation with a beam current of $2 \times 10^{-7}\,A$, which was monitored by detecting the probe current between the sample stage and the beam filament.[16] Welding was performed at several sites on each electrode. As the result, contact resistance decreased dramatically from $10-100\,k\Omega$ to a value below the sample resistance
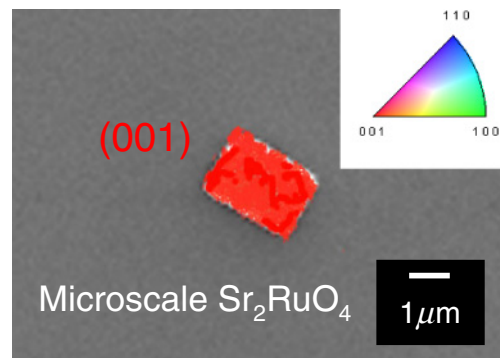
Fig. 2. (Color online) Result for microscale Sr_2RuO_4 single crystal (sample B) measured using the electron backscatter diffraction pattern. The color variations of the inset represent the crystal orientations. The red region shows a single crystal in the *ab*-plane.
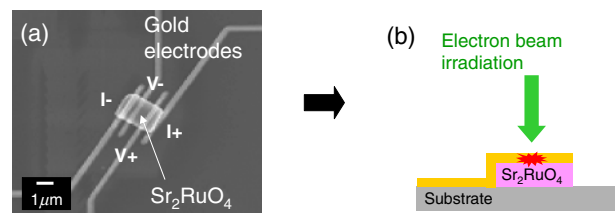
Fig. 3. (Color online) (a) Micrograph of sample B connected to gold electrodes. (b) Schematic of welding by electron beam irradiation.

at room temperature. We confirmed that contact resistance did not increase with decreasing temperature. The fabricated samples were cooled to low temperatures several times, and kept there to form electrical contact with gold electrodes.

The measurements were performed in a dilution refrigerator (Oxford Kelvinox) with a base temperature of $60\,mK$. All measurement leads were shielded. The lead lines were equipped with low-pass resistance–capacitance filters ($R = 1\,k\Omega$, $C = 22\,nF$). Silver wires $50\,\mu m$ in diameter were attached to the gold contact pads using a silver paste. In the DC measurements, a bias current was supplied using a precise current source (Keithley 6220) and the voltage was measured with a nanovoltmeter (Keithley 182) via four-terminal measurements.

We observed the superconducting properties of microscale Sr_2RuO_4. Figure 4(a) shows the superconducting transition temperature $T_c = 1.59\,K$ and transition temperature width $\Delta T \approx 30\,mK$ in zero magnetic field. We measured the temperature dependence of resistivity for bias current $I = \pm1\,\mu A$ by the current reversal method. The properties of sample A are consistent with the properties of bulk Sr_2RuO_4 single crystals.[13] Figure 4(b) shows $T_c = 1.69\,K$ and $\Delta T \approx 200\,mK$. The resistivity of sample B retained its flat tail below T_c. We consider that a finite resistivity shows a flow of vortices owing to quantum fluctuations of the phase θ.[17,18] These results indicate that we were successful in observing the superconducting properties of the synthesized and selected microscale Sr_2RuO_4 single crystals. The procedure will promote fundamental studies of spin-triplet chiral p-wave Sr_2RuO_4 and its potential applications to topological quantum
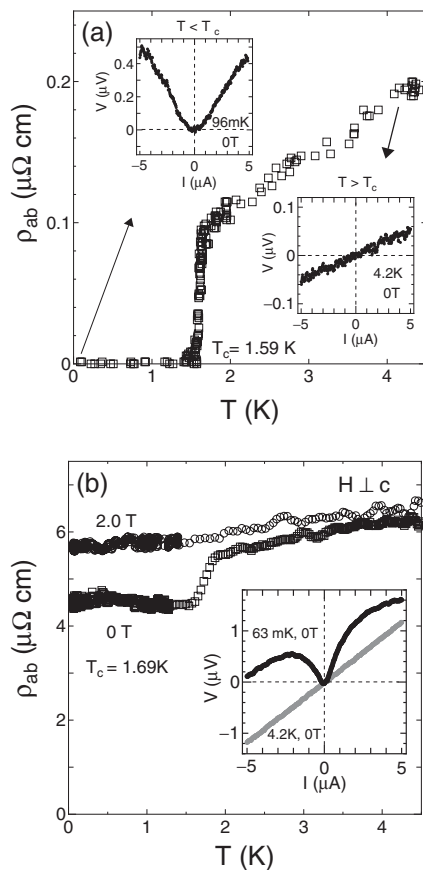
Fig. 4. Temperature dependence of resistivity of microscale Sr_2RuO_4. (a) Sample A shows zero resistivity in zero magnetic field. (b) A finite resistivity is seen in sample B below T_c. Insets show the results of DC measurements. Above T_c, the I–V curve shows ohmic conduction. In contrast, below T_c, an anomalous I–V curve is observed. We eliminated offset voltage. The anomalous behavior is reproduced in both samples.

computation. The procedure can also be adjusted in studies of microscale single crystals in anisotropic superconductors such as copper-based and recently reported iron-based materials.

Furthermore, in both samples A and B, we observed anomalous current–voltage (I–V) characteristics. In general, the induced voltage V is an odd function of the bias current I. The I–V curves show ohmic conduction above T_c [see inset of Figs. 4(a) and 4(b)]. However, below T_c, the results show that V is an even function of I. With decreasing temperature, anomalous voltage increases in zero magnetic field. With increasing magnetic field, anomalous voltage decreases at low temperature. We measured the differential resistance dV/dI as a function of I in the AC measurements. The effect has been confirmed in both DC and AC measurements.[10] More importantly, the anomalous behavior is reproduced in both samples A and B. We consider that the anomalous induced voltage clearly exhibits a property of the single chiral domain because our sample size is comparable

to the single domain scale. The phenomenon is related to phase slip, which is caused by quantum fluctuations in microscale superconductors.[19] To understand the anomalous effect, we suggested an unconventional vortex model in the single domain of Sr_2RuO_4.[10] We need to further study the transport properties of microscale Sr_2RuO_4 single crystals.

In summary, we studied the transport properties in a single chiral domain of microscale Sr_2RuO_4 single crystals. Microscale Sr_2RuO_4 single crystals were selected by detailed analyses. To measure the transport properties, gold electrodes were firmly attached to the crystals by welding with electron beam irradiation. The microscale Sr_2RuO_4 showed the superconducting properties. Anomalous I–V characteristics were observed.

1) J. G. Bednorz and K. A. Müller: Z. Phys. B **64** (1986) 189.
2) Y. Maeno, H. Hashimoto, K. Yoshida, S. Nishizaki, T. Fujita, J. G. Bednorz, and F. Lichtenberg: Nature **372** (1994) 532.
3) Y. Kamihara, H. Hiramatsu, M. Hirano, R. Kawamura, H. Yanagi, T. Kamiya, and H. Hosono: J. Am. Chem. Soc. **128** (2006) 10012.
4) A. P. Mackenzie and Y. Maeno: Rev. Mod. Phys. **75** (2003) 657.
5) J. Xia, Y. Maeno, P. T. Beyersdorf, M. M. Fejer, and A. Kapitulnik: Phys. Rev. Lett. **97** (2006) 167002.
6) F. Kidwingira, J. D. Strand, D. J. V. Harlingen, and Y. Maeno: Science **314** (2006) 1267.
7) C. Nayak, S. H. Simon, A. Stern, M. Freedman, and S. D. Sarma: Rev. Mod. Phys. **80** (2008) 1083.
8) H. Kambara, S. Kashiwaya, H. Yaguchi, Y. Asano, Y. Tanaka, and Y. Maeno: Phys. Rev. Lett. **101** (2008) 267003.
9) H. Yaguchi, K. Takizawa, M. Kawamura, N. Kikugawa, Y. Maeno, T. Meno, T. Akazaki, K. Semba, and H. Takayanagi: J. Phys. Soc. Jpn. **75** (2006) 125001.
10) H. Nobukane, K. Inagaki, K. Ichimura, K. Yamaya, S. Takayanagi, I. Kawasaki, K. Tenya, H. Amitsuka, K. Konno, Y. Asano, and S. Tanda: Solid State Commun. **149** (2009) 1212.
11) P. Mohanty, J. Y. T. Wei, V. Ananth, P. Morales, and W. Skocpol: Physica C **408** (2004) 666.
12) F. Lichtenberg, A. Catana, J. Mannhart, and D. G. Schlom: Appl. Phys. Lett. **60** (1992) 1138.
13) A. P. Mackenzie, R. K. Haselwimmer, A. W. Tyler, G. G. Lonzarich, Y. Mori, S. Nishizaki, and Y. Maeno: Phys. Rev. Lett. **80** (1998) 161.
14) K. S. Novoselov, D. Jiang, F. Schedin, T. J. Booth, V. V. Khotkevich, S. V. Morozov, and A. K. Geim: Proc. Natl. Acad. Sci. U.S.A. **102** (2005) 10451.
15) B. L. Adams, S. I. Wright, and K. Kunze: Metall. Trans. A **24** (1993) 819.
16) K. Inagaki, T. Toshima, S. Tanda, and K. Yamaya: Appl. Phys. Lett. **86** (2005) 073101.
17) E. Chow, P. Delsing, and D. B. Haviland: Phys. Rev. Lett. **81** (1998) 204.
18) H. M. Jaeger, D. B. Haviland, B. G. Orr, and A. M. Goldman: Phys. Rev. B **40** (1989) 182.
19) M. Tinkham: *Introduction to Superconductivity* (McGraw-Hill, New York, 1975) Chap. 8.